Pure Appl. Geophys.

DOI 10.1007/s00024-017-1660-5

Pure and Applied Geophysics

Numerical Procedure to Forecast the Tsunami Parameters from a Database of Pre-Simulated Seismic Unit Sources

César Jiménez,[1,2] Carlos Carbonel,[1] and Joel Rojas[1]

Abstract—We have implemented a numerical procedure to forecast the parameters of a tsunami, such as the arrival time of the front of the first wave and the maximum wave height in real and virtual tidal stations along the Peruvian coast, with this purpose a database of pre-computed synthetic tsunami waveforms (or Green functions) was obtained from numerical simulation of seismic unit sources (dimension: 50×50 km^2) for subduction zones from southern Chile to northern Mexico. A bathymetry resolution of 30 arc-sec (approximately 927 m) was used. The resulting tsunami waveform is obtained from the superposition of synthetic waveforms corresponding to several seismic unit sources contained within the tsunami source geometry. The numerical procedure was applied to the Chilean tsunami of April 1, 2014. The results show a very good correlation for stations with wave amplitude greater than 1 m, in the case of the Arica tide station an error (from the maximum height of the observed and simulated waveform) of 3.5% was obtained, for Callao station the error was 12% and the largest error was in Chimbote with 53.5%, however, due to the low amplitude of the Chimbote wave (<1 m), the overestimated error, in this case, is not important for evacuation purposes. The aim of the present research is tsunami early warning, where speed is required rather than accuracy, so the results should be taken as preliminary.

Key words: Tsunami, numerical simulation, forecasting.

1. Introduction

According to historical seismicity (Silgado 1978; Beck and Nishenko 1990), many destructive earthquakes have occurred in Peru. Some of which have generated tsunamis that have affected ports and coastal towns, for instance, the remarkable tsunami of Callao 1746 in central Peru (Dorbath et al. 1990; Jiménez et al. 2013; Mas et al. 2014a) and the tsunami of southern Peru in 1868, both megathrust earthquakes with a magnitude around M_w 9.0. In the twentieth century, there were the tsunamigenic earthquakes of 1960 in Lambayeque (M_w 7.6), 1966 in northern Lima (M_w 8.1), 1974 in southern Lima (M_w 8.1) (Beck and Ruff 1989), 1996 in Chimbote (M_w 7.5) and 1996 in Nazca (M_w 7.7). According to instrumental seismicity (after 1960), only in the twenty-first century there have been two major tsunamigenic earthquakes in Peru: Camana in 2001 (M_w 8.4) (Adriano et al. 2016) and Pisco in 2007 (M_w 8.1) (Jiménez et al. 2014). Accordingly, regarding tsunami hazard, the main issue in Peru is the near-field tsunami event, where the tsunami arrival time is in the range of 15–60 min (Mas et al. 2014b). Therefore, it is necessary to develop a system to forecast, in the shortest possible time, the tsunami parameters from a database of pre-simulated seismic unit sources.

The "Centro Nacional de Alerta de Tsunamis" from Peru (CNAT in Spanish, corresponding to Peruvian Tsunami Warning Center) is the official representative to international institutions such as the Pacific Tsunami Warning Center (PTWC), responsible for issuing information bulletins, alert or alarm in case of occurrence of tsunamis for near-field or far-field origin. For near-field events, it is not convenient to compute a numerical tsunami simulation immediately after the occurrence of an earthquake because this process may take several hours and the arrival time is in order of the minutes. For this purpose, it is required to process quickly and accurately the seismic information (hypocenter location and magnitude) provided by the Instituto Geofísico del Perú (IGP) for earthquakes generated in the near field (local) or by USGS (United States Geological Survey) for earthquakes generated in the far field. To accelerate the processing of information is necessary to implement

[1] Laboratorio de Física de la Tierra, Universidad Nacional Mayor de San Marcos, Av. Germán Amézaga N° 375, Lima 1, Peru. E-mail: cjimenezt@unmsm.edu.pe

[2] Centro Nacional de Alerta de Tsunamis, Dirección de Hidrografía y Navegación, Jr. Roca 118, Callao, Peru.

Published online: 04 September 2017

some numerical procedure to process such information automatically from a database of pre-computed tsunami scenarios.

1.1. State of the Art

As research antecedents, Gica et al. (2008), implemented a database of pre-calculated seismic events to forecast tsunami parameters (arrival time, maximum tsunami height) with seismic unit sources of 50 × 100 km^2 using a bathymetry of 4 arc-min resolution. This system is used by the National Oceanic and Atmospheric Administration (NOAA) and this pre-computed database serves as input to an intermediate resolution model along the coast. On the other hand, Greenslade et al. (2011) implemented a model to forecast tsunamis from a database of seismic scenarios, which is used by the Tsunami Warning Center in Australia for buoys at offshore (not for tidal gauges on the coast), the bathymetry resolution is 4 arc-min and the size of the seismic source is 100 × 100 km^2.

Jiménez (2010) presented a numerical procedure to determine the occurrence of tsunamis based on hypocentral parameters and magnitude. Also, an algorithm to calculate quickly the arrival time of the first tsunami wave (based on a linear trajectory followed by the tsunami wave according to actual bathymetry) was implemented. That research was the starting point for the next step: the calculation of the tsunami wave height from tsunami numerical modeling.

In the present paper, the results of Jiménez (2010) are extended to calculate the arrival time of the front of the first tsunami wave and the maximum wave height (of the whole computation time) for real and virtual coastal tide gauge stations. This is based on a database or catalogue of synthetic tsunami waveforms (or Green functions) obtained by tsunami numerical simulation of unitary seismic sources of dimensions 50 × 50 km^2, unitary dislocation with a focal mechanism based on Global Centroid Moment Tensor (CMT) catalogue and a 5 km depth for the shallower end of the subfault that is near the trench. The bathymetry has a grid resolution of 30 arc-sec (approximately 927 m). Hence, this paper covers important and interesting work being undertaken to develop a tsunami scenario database for Peru. It will provide a tool that can be used to determine if tsunami warnings are needed for parts of the Peruvian coastline.

2. Data

2.1. Bathymetry Data

The tsunami wave speed and directivity depend on bathymetry; therefore, a good description of bathymetry is important to conduct numerical simulation of propagation of tsunamis. The global bathymetry model is taken from GEBCO 30 (2017), which has a grid resolution of 30 arc-sec or approximately 927 m. The fine bathymetry in coastal zones has been updated from marine soundings provided by the Directorate of Hydrography and Navigation (DHN) of the Peruvian Navy. Figure 1 shows the bathymetry of the whole Pacific Ocean, the seismicity for 2015 and the principal subduction zones.

2.2. Focal Mechanism Parameters and Seismicity

The focal mechanism parameters (azimuthal or strike angle θ, dip angle δ, and rake angle λ) are taken from historical averages of the catalogue of the Global Centroid Moment Tensor (CMT) for a given subduction zone, (http://www.globalcmt.org, last accessed: December 2015). In some cases, the strike angle is taken according to the orientation of the trench or parallel to the coast, also the rake or dislocation angle is taken as 90° to obtain a maximum vertical seafloor deformation. The upper side depth of the subfault near the trench is taken as 5 km; according to dip angle, the intermediate depth subfault is set to 17–21 km and the depth of the subfault close to coast is around 30 km.

To define the computational grid, it is necessary to know the location of the subduction zones in the Pacific Ocean. From seismicity data and focal mechanism parameters is possible to deduce the seismic subduction zones along the Pacific Ocean. These subduction zones contain: Chile, Peru to Central America up to northern Mexico, Cascadia zone, Alaska, Aleutians islands, Kuril Islands, Japan, Marianas trench, Tonga and Kermadec (Fig. 1).

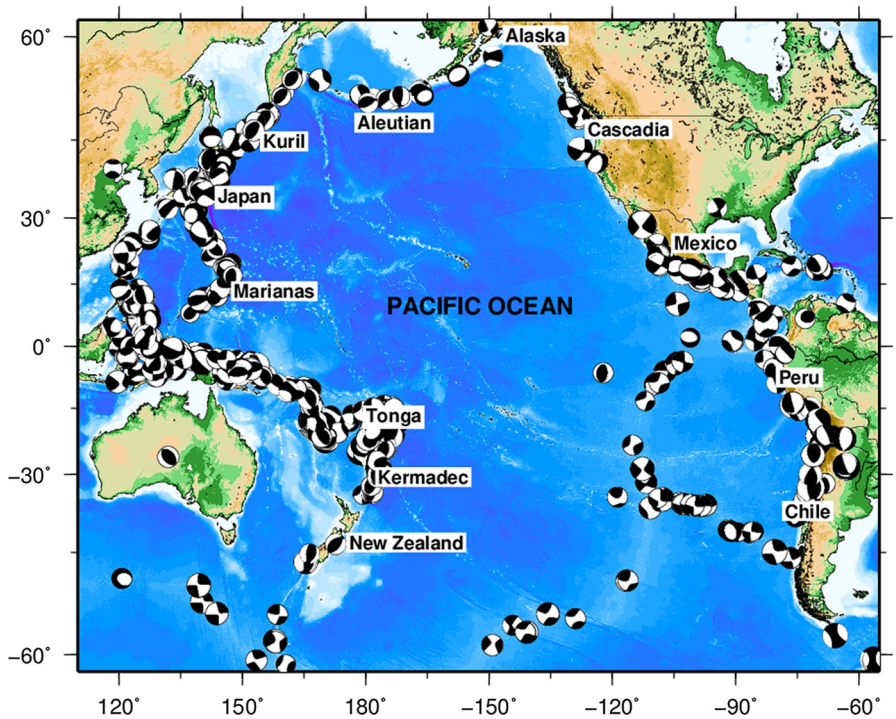

Figure 1
Bathymetry of the Pacific Ocean from GEBCO 30. The *circles* represent the focal mechanism of seismic events ($M_w > 5.0$) of 2015 from Global CMT catalogue. The tags represent the principal subduction zones

3. Methodology

The methodology could be summarized in the following form: First, the coseismic deformation must be calculated and used as the initial condition for the tsunami wave propagation. Later, a database or catalogue of synthetic tsunami waveforms was implemented from tsunami numerical simulation of unitary seismic sources.

3.1. Coseismic Deformation

The initial condition for tsunami propagation is calculated using the deformation model of Okada (1992) for an elastic, homogeneous and isotropic semi-infinite medium. Seismic sources are considered of dimensions 50×50 km^2, unitary dislocation (slip = 1 m) and depth of the upper side of the shallower unit source is 5 km; the depths of the deeper unit sources will depend on the dip angle and the width (50 km, in this case) of the unit source. The focal mechanism parameters are taken from the mean values of the CMT catalogue and the seismicity of the corresponding subduction zone (from southern Chile to northern Mexico).

We assume that the generation of coseismic deformation of the seafloor produces an immediate and identical deformation on the ocean surface (due to the incompressibility of the fluid). As the ocean is a fluid, the deformation does not hold its shape and the initial displacement radiates away from the source creating a tsunami wave that propagates in all directions (Okal 2009). Figure 2 shows an example of deformation field.

3.2. Tsunami Numerical Modeling

A modified version of TUNAMI-F1 (IOC-Intergovernmental Oceanographic Commission 1997) numerical model was used. This code was written in Fortran. The algorithm corresponds to a linear model in a regular grid-system using spherical

coordinates based on shallow water theory. The differential equations (linear momentum conservation and mass conservation or continuity equation) are integrated numerically using the method of "leap frog" in a finite differences scheme. A numerical stability condition (CFL condition) of less than 0.8 was used to avoid numerical instabilities.

The initial conditions are based on the deformation theory by Okada (1992). The boundary conditions along the coastline (for the linear model) represent a vertical wall, so we suggest the use of a correction factor for the synthetic tsunami waveform of each tidal station (to approximate a non-linear system).

The numerical code is written in Fortran and runs in a Linux system. The digital processing of input data and output results was made in Matlab. The graphical user interface (GUI) was implemented also in Matlab. The final application runs under Windows or Linux.

3.3. Unitary Seismic Sources and Green Functions

The set of unitary seismic sources and tsunami waveforms form the database of the model. The number of unitary seismic sources is proportional to the geographical extent of the database. Therefore, the chances of predicting the tsunami parameters of an earthquake generated somewhere in the Pacific Ocean will be greater.

Taking into account the seismicity of the Peruvian coast and adjacent countries, the computational domain was initially chosen from Antofagasta (Chile) to Ecuador. For the first stage, this area has been divided into 130 "unit seismic sources" of dimensions 50×50 km^2. The idea is to simulate the propagation of tsunami waveforms for each seismic unit source and calculate the Green functions $G(t)$ or synthetic mareograms at each port and coastal town in Peru, where real and virtual tide gauge stations have been selected. Currently and in a second stage, 465 seismic unit sources have been modeled, from southern Chile to northern Mexico.

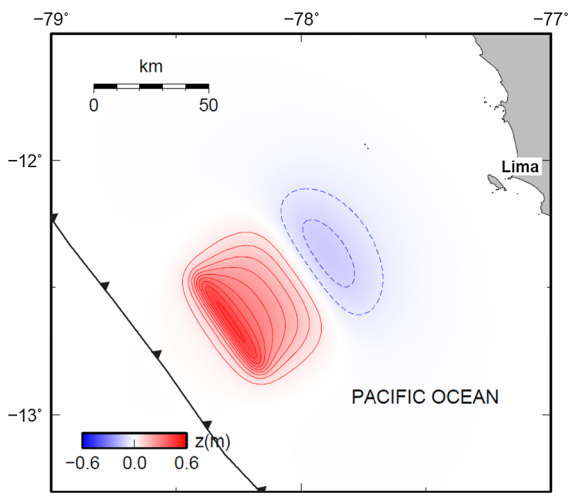

Figure 2
Example of coseismic deformation field of a unitary seismic source located offshore Lima. The *red color* represents the uplift and *blue color* represents subsidence. The *barbed lines* represent the Peruvian trench

3.4. Virtual Tidal Stations

There are 17 numerical tide gauge station within the computational area, many of them correspond with the actual location of real tidal stations. These virtual stations correspond to ports and coastal towns (Fig. 3). The geographical coordinates and the empirical correction factor of each station are shown in Table 1.

A major aspect of the database is the development of correction factors for each individual tidal station. These correction factors account for the amplification or attenuation of the tsunami waves in shallow waters due to non-linear processes that cannot be simulated using linear model. These correction factors are determined in an empirical way as the rate of the maximum observed tsunami height over the maximum simulated tsunami height.

3.5. Governing Equations of the Numerical Model

All the equations are highly dependent on earthquake magnitude Mw and epicenter location. According to scaling laws between the dimensions of a fault plane or seismic source (of rectangular geometry) and the magnitude of the earthquake for subduction zones (Papazachos et al. 2004), we have the basic empirical relations

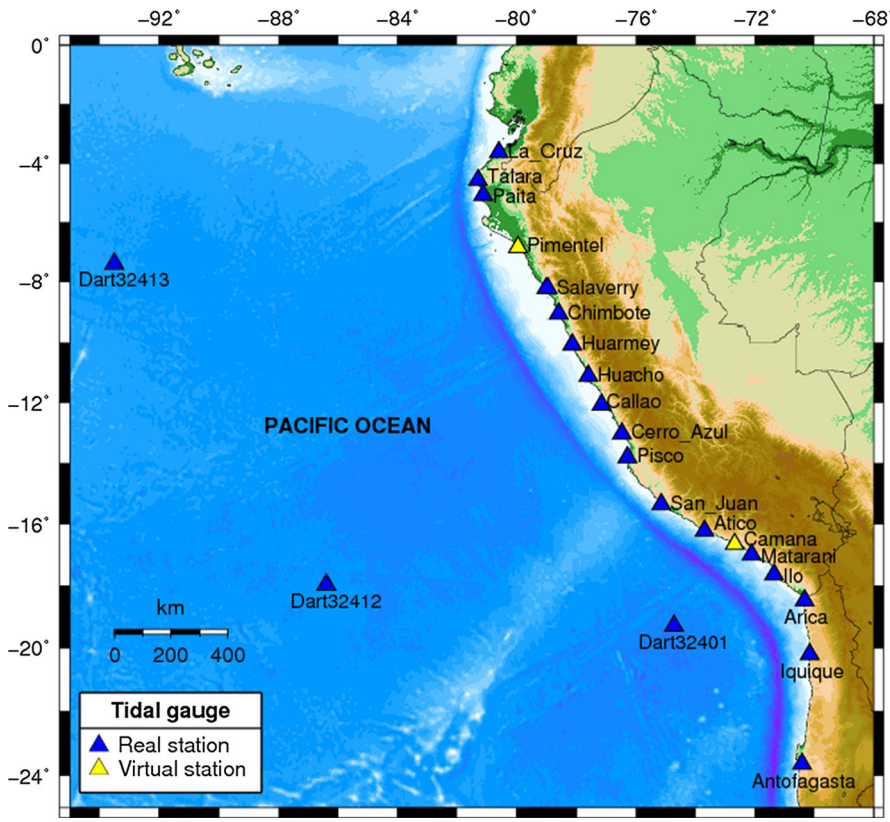

Figure 3
Location of virtual and real tide gauge station to be considered in the numerical modeling

$$\log(L) = 0.55M - 2.19 \quad (1)$$

$$\log(W) = 0.31M - 0.63, \quad (2)$$

where L is the length (in km) of the seismic source, W is the width (in km) of the seismic source, and M is the moment magnitude (M_w). The seismic moment defined by (Aki 1966) is

$$M_0 = \mu LWD, \quad (3)$$

where μ is the mean rigidity modulus (4×10^{10} N/m^2) of the rupture zone and D is the dislocation or slip of the seismic source. The relationship between seismic moment (in N × m) and the moment magnitude is given by the relation,

$$\log(M_0) = 1.5M_w + 9.1. \quad (4)$$

The model output (tsunami waveform) is the linear combination of the synthetic tsunami waveforms or Green functions $G(t)$ corresponding to the seismic unit sources contained in the rupture geometry (Fig. 4). The number of seismic unit sources is given by

$$N = \frac{LW}{L_0 W_0}, \quad (5)$$

where $L_0 = 50$ km, $W_0 = 50$ km, corresponding to the dimensions of the unitary seismic source. Therefore, for an earthquake of M_w 7.0 only one seismic source is required, but for an earthquake of M_w 8.0, 5 seismic sources are required (Table 2). The criterion in selecting the deeper or shallower unit seismic source is based on an algorithm that takes into account the nearest distance from the epicenter. Also, an amplification factor is required: the dislocation or mean slip D. To linearize the model, an empirical correction factor K_i for each coastal tidal station is required. The signal of the tsunami $f_i(t)$ in i-th tidal station is given by

Table 1

Location of real and virtual tidal stations used in the numerical simulation

N	Station	Lat (°)	Lon (°)	K_i
1	La Cruz	−03.6337	−80.5876	0.74
2	Talara	−04.5751	−81.2827	0.88
3	Paita	−05.0837	−81.1077	0.94
4	Pimentel	−06.8396	−79.9423	0.75
5	Salaverry	−08.2279	−78.9818	0.70
6	Chimbote	−09.0763	−78.6128	0.46
7	Huarmey	−10.0718	−78.1616	1.05
8	Huacho	−11.1218	−77.6162	0.95
9	Callao	−12.0689	−77.1667	0.80
10	Cerro Azul	−13.0253	−76.4808	0.82
11	Pisco	−13.8061	−76.2919	0.65
12	San Juan	−15.3556	−75.1603	0.60
13	Atico	−16.2311	−73.6944	1.00
14	Camaná	−16.6604	−72.6838	0.40
15	Matarani	−17.0009	−72.1088	0.80
16	Ilo	−17.6445	−71.3486	0.79
17	Arica	−18.4758	−70.3232	0.70

The parameter K_i represents the empirical correction factor that takes into account the linearity

$$f_i(t) = DK_i \sum_{j=1}^{N} G_{ij}(t), \tag{6}$$

where G_{ij} (t) is the Green function (synthetic tsunami waveform) for the i-th tidal station due to the j-th seismic unit source.

4. Results

4.1. Graphical User Interface: "Pre-Tsunami"

With the information of hypocentral parameters, conditions of tsunami generation and algorithm of pre-computed seismic unit sources, we have implemented an application with a graphical user interface developed in Matlab programming language. The input data are the hypocentral parameters: magnitude M_w, hypocentral depth (this is used for discriminating the sources greater than 60 km depth), geographical latitude and longitude of the epicenter and origin time. The outputs are the parameters of seismic source geometry and a diagram of the likely rupture geometry on a map.

The subroutine "Arrival Time" calculates the arrival times from the dependence of wave velocity with respect to the bathymetry. The subroutine "Catalogue" calculates the arrival time of the front of the first wave and the maximum wave height of the tsunami (Fig. 5) in ports and coastal towns of Peru, from a database of synthetic tsunami waveforms or Green functions. The time of calculation is very fast, in the order of a few seconds due to the pre-calculated synthetic tsunami waveforms.

The subroutine "Automatic IGP" loads the hypocentral parameters from the website of the seismological service of IGP (Instituto Geofísico del Perú, in spanish) to avoid the manual introduction of these parameters in the case of some big earthquake in the near field reported by the Peruvian seismological service of IGP.

The graphical user interface of Pre-Tsunami application is quite friendly and easy to use by the operator of the tsunami warning and constitutes an important computational tool to forecast and decision making for issuing bulletins, alert or alarm in case of occurrence of tsunamis. The last version (V4.6) was updated in August 2016 (Fig. 6).

4.2. Output of the Application Pre-Tsunami

The output of the model will be useful to forecast tsunamis in the near, regional and far field. The output parameters are: the arrival time of the front of the first wave and the maximum height of the tsunami wave. These results will be useful for issuing the alert or alarm of the tsunami. For example, for a hypothetical M_w 8.6 magnitude earthquake with epicenter offshore of Lima (Lat = −12.00°, Lon = −78.00°, Depth = 20 km, origin time: 00:00), according to the threshold of tsunami heights of PTWC, maximum evacuation ($H_{max} > 3$ m) would be declared for Huacho, Callao and Cerro Azul (Table 3).

4.3. Application to the Tsunami of Chile 2014 (M_w 8.2: USGS Preliminary Report)

A big earthquake and tsunami was generated in Iquique Chile on 01 April 2014 (Lay et al. 2014; An et al. 2014). The hypocentral parameters (longitude, latitude, depth and origin time) reported by NEIC-USGS (http://earthquake.usgs.gov/earthquakes/map/)

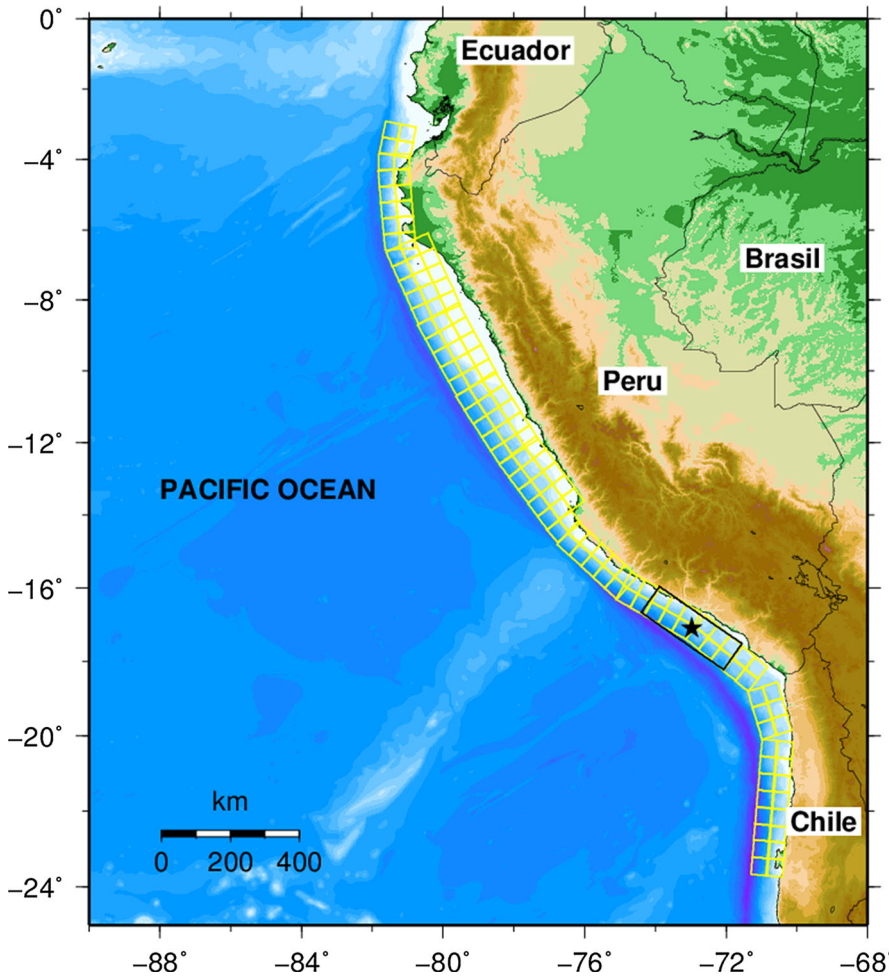

Figure 4
Location of unit seismic sources and an example of a major earthquake (*black rectangle*). The *black star* represents the epicentroid (gravity center of the seismic source)

were: lon = −70.817°, lat = −19.642°, $z = 25$ km, origin time: 23:46:46 UTC.

The acquisition of data from the National Tide Gauge Network of Peru (http://www.dhn.mil.pe) and Arica Station (tide gauge from Chilean network, available on: http://www.ioc-sealevelmonitoring.org) was performed. Digital signal processing was performed for these signals; a high-pass Butterworth filter with cut frequency: $f_c = 6.94 \times 10^{-5}$ Hz and a low-pass filter ($f_c = 0.0083$ Hz) was applied to remove components of long period (tides) and short period (surges); so, the maximum amplitude of the tsunami wave was calculated (Table 4). The calculation of the parameters of the simulated tsunami was conducted using the Pre-Tsunami application (version 4.6). This event has allowed calibrating the values of the correction factor K_i for each station.

The results show a very good correlation for stations with wave amplitude greater than 1 m, meanwhile for Pisco and Chimbote stations the correlation is poor. For the case of Arica station, the error was of 3.5% and Ilo's error was 5.7%. In the case of Callao station, the error was 12% and the largest error was in Pisco (34.8%) and Chimbote (53.5%). This does not mean that the method presented is flawed and not useful, rather it shows the limitations of the numerical method. With additional data from DART buoys and future

Table 2

Number of unit sources N required according to the magnitude of the earthquake

Magnitude (M_w)	N
7.0	1
7.5	2
8.0	5
8.5	12
9.0	32

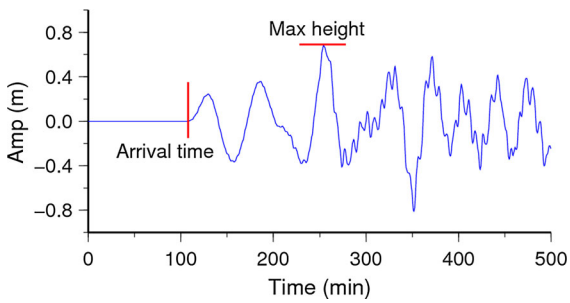

Figure 5
Diagram showing a synthetic tsunami waveform. The *vertical red line* represents the arrival time and the *horizontal red line*, the maximum tsunami height

tsunamis, updating and calibration of Pre-Tsunami application will be performed (i.e., the empirical correction factors of each tidal station), achieving on the future a greater reliability. Additionally, due to the low amplitude of the Pisco and Chimbote wave (<1 m), the overestimated error is not important for evacuation purposes.

4.4. Projection of the Catalogue of Seismic Unit Sources

The current addition in the database of the simulation is shown in Fig. 7, geographically, from southern Chile to northern Mexico with 465 seismic unit sources simulated. We hope to conduct the simulation of seismic unit sources for the entire Pacific Ocean corresponding to subduction zones of Pacific Seismic Ring. This implies a large computational effort with the simulation of more than 1000 seismic unit sources, for a computational grid around the Pacific Ocean with 30 arc-sec resolution or 1 min resolution for the far field.

The Directorate of Hydrography and Navigation (DHN) of the Peruvian Navy have acquired, at beginning of 2016, a high-performance computer or cluster with 32 cores or processors for scientific numerical calculations to conduct these tsunami numerical simulations. The computation time will be considerably reduced with the use of this high-performance computer: each seismic unit source simulation is computed in approximately 30 min for a computational grid of 3720 × 5760 elements, while this very computation lasted more than 3 h in a personal computer with microprocessor i7 of 3.40 GHz.

In the future, we expect to conduct the inversion of tsunami waveforms to obtain the distribution of the seismic source.

5. Discussion

5.1. Limitations of the Model

A linear model is used to simulate a non-linear phenomenon, for this reason we suggest the use of an empirical correction factor for each tidal station. This correction factor must be calibrated with every new tsunami event.

The model is strongly dependent on the seismic magnitude and epicenter location. In addition, the model takes the mean values of the focal mechanism CMT catalogue, if the variation of focal mechanism is great, the forecast will not be very good.

In most of the cases, if the epicenter does not match with the epicentroid, the results will be biased due to the position of the seismic source. It is difficult to obtain the geometry of the seismic source immediately after the occurrence of the earthquake; this issue can be resolved with the aftershock distribution, many hours later.

For the far field, the numerical model does not take into account the effects of dispersion, which is a non-linear effect. The model assumes homogeneous and regular deformation; the reality is that the seismic source can have a heterogeneous asperity distribution.

5.2. Strengths of the Model

The time that the application spends to provide the tsunami parameters is immediate, since it has a

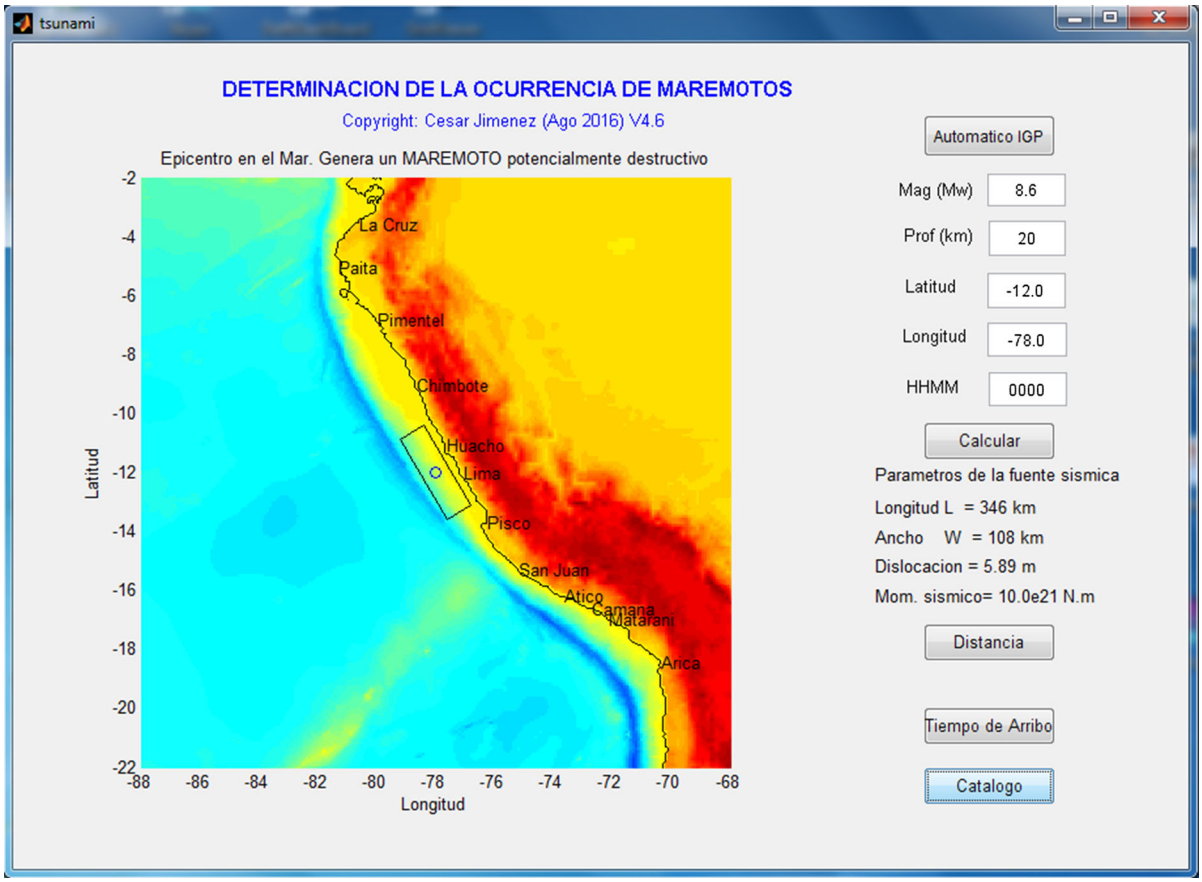

Figure 6
Graphical user interface pre-tsunami (Version 4.6)

database of simulations previously computed. The model works well when the epicenter matches with the epicentroid or gravity center of the rupture geometry, as the case of Chile earthquake of 2014.

This model is applicable for seismic events in the near and regional field, due to the reaction time is in the order of a few minutes to 1 h. On the other hand, for tsunamis in the far field, the forecaster has a greater reaction time, in the order of many hours.

The GUI (Graphical User Interface) is user friendly and easy to use by an operator (it is not necessary the operator be an expert in programming or numerical simulation). As a post-tsunami analysis, the Green functions of the model can be used to obtain the distribution of the seismic source, with an inversion calculation.

We have mentioned that this model requires the aftershock distribution to solve the location of the seismic source. Therefore, in a real application, the accuracy of this system without knowing the real rupture geometry is good, from the point of view of the tsunami early warning operator.

6. *Summary and Conclusions*

We have presented a numerical procedure to determine quickly the occurrence of a tsunami and to forecast some parameters: the arrival time of the front of the first tsunami wave and the maximum tsunami wave height in the different coastal cities. The application “Pre-Tsunami” is of practical use in the Peruvian Tsunami Warning Center.

The numerical model tries to reproduce a physical process (as is the process of interaction of tsunami waves near the coast) through a linear simulation

Table 3

Output of the numerical model: arrival time T_A and maximum wave height H_{max}

Port	Region	T_A	H_{max} (m)
La Cruz	N	01:54	0.26
Talara	N	01:05	0.12
Paita	N	01:15	0.52
Pimentel	N	01:42	0.95
Salaverry	N	01:34	2.70
Chimbote	C	01:11	1.39
Huarmey	C	00:22	2.32
Huacho	C	00:20	3.41
Callao	C	00:24	6.75
Cerro Azul	C	00:37	3.35
Pisco	C	00:40	2.10
San Juan	C	00:43	0.91
Atico	S	00:55	0.28
Camaná	S	01:15	0.28
Matarani	S	01:09	0.18
Ilo	S	01:22	0.40
Arica	S	01:39	0.59

Region: Northern (N), Central (C) and Southern (S)

Table 4

Comparison of the observed and simulated maximum tsunami wave heights at gauge sites for Chilean earthquake and tsunami of 01 April 2014

Station	Observed (m)	Simulated (m)	% Error
Arica	2.00	2.07	3.5
Ilo	1.05	1.11	5.7
Matarani	0.52	0.60	15.4
San Juan	0.45	0.51	13.3
Pisco	0.23	0.31	34.8
Callao	0.25	0.28	12.0
Chimbote	0.15	0.23	53.5
Salaverry	0.20	0.18	(−) 10.0
Paita	0.10	0.11	10.0

Negative values (−) indicate underestimation

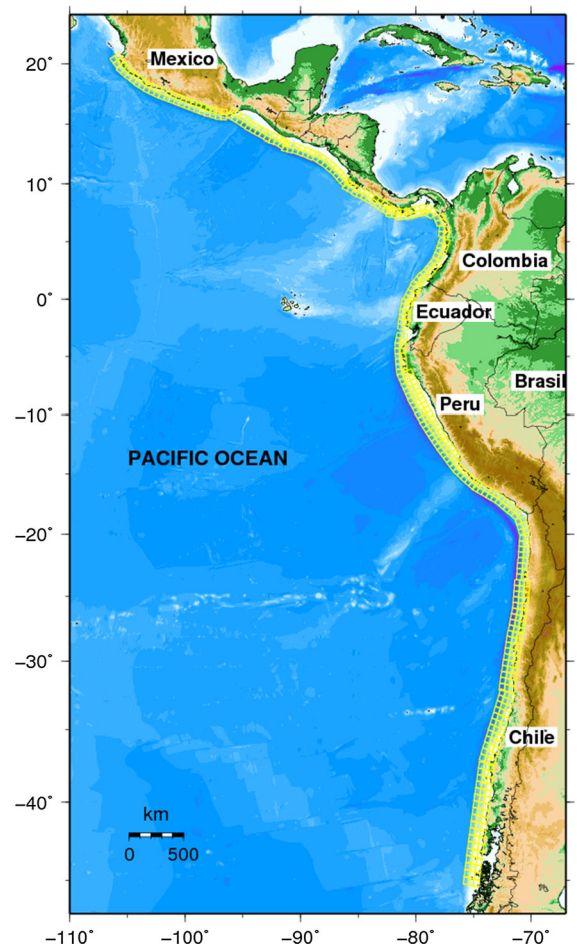

Figure 7
The small *yellow squares* represent the unitary pre-calculated seismic sources. The advance covers the subduction zone from southern (Chile) to northern Mexico with 465 seismic sources

model (as is the process of propagation of the tsunami) to use the principle of superposition of the Green functions. This could suggest the use of a "linearity correction factor" for each tidal station, which can be empirically calibrated and updated with each new tsunami event.

Despite the limitations of the model, the results are of practical use as a first approximation for purposes of fast estimation of tsunami parameters to issue the alerts and warnings of tsunamis in the near field, due to the speed with which the tsunami parameters are obtained.

The application of the model to the earthquake and tsunami in northern Chile 2014 (M_w 8.2) indicates a very good correlation between the maximum heights of observed and simulated waves for amplitudes greater than 1 m. In the case of tidal station of Arica (amplitude = 2.0 m), the error was 3.5%; for Ilo station (amplitude = 1.05 m), the error was 5.7%; Callao's error was 12%. The largest error was in Chimbote with 53.5%, however, due to the low amplitude of the Chimbote wave (<1 m), the overestimated error is not important for evacuation

purposes. We must take into account that the aim of the research is tsunami early warning, where speed is required rather than accuracy.

Acknowledgements

This research was sponsored in part by the Vicerectorate for Research and Postgraduate from "Universidad Nacional Mayor de San Marcos" (Group Research Project 2017) and by the "Direccion de Hidrografia y Navegacion" from Peruvian Navy. In addition, we acknowledge the anonymous reviewers.

References

Adriano, B., Mas, E., Koshimura, S., Fujii, Y., Yanagisawa, H., & Estrada, M. (2016). Revisiting the 2001 Peruvian earthquake and tsunami impact along Camana beach and the coastline using numerical modeling and satellite imaging. In: Chapter I of Tsunamis and earthquakes in coastal environments Springer Int. doi:10.1007/978-3-319-28528-3_1.

Aki, K. (1966). Estimation of earthquake moment, released energy, and stress-strain drop from the G wave spectrum. *Bulletin Earthquake Research Institute, 44,* 73–88.

An, C., Sepúlveda, I., & Liu, P. L.-F. (2014). Tsunami source and its validation of the 2014 Iquique, Chile Earthquake. *Geophysical Research Letters, 41,* 3988. doi:10.1002/2014GL060567.

Beck, S., & Nishenko, S. (1990). Variations in the mode of great earthquake rupture along the Central Peru subduction zone. *Geophysical Research Letters, 17*(11), 1969–1972.

Beck, S., & Ruff, L. (1989). Great earthquakes and subduction along the Peru trench. *Physics of the Earth and Planetary Interiors, 57,* 199–224.

Dorbath, L., Cisternas, A., & Dorbath, C. (1990). Assessment of the size of large and great historical earthquakes in Peru. *Bulletin of Seismological Society of America, 80*(3), 551–576.

GEBCO 30. (2017). General Bathymetric Chart of the Oceans. Web: http://www.gebco.net. Accessed Nov 2016.

Gica, E., Spillane, E., Titov, V., Chamberlin, C., & Newman, J. (2008). Development of the forecast propagation database for NOAA's short-term inundation forecast for Tsunamis (SIFT). NOAA Technical Memorandum OAR PMEL-139, pp 89.

Greenslade, D., Allen, S., & Simanjuntak, M. (2011). An evaluation of tsunami forecasts from the T2 scenario database. *Pure and Applied Geophysics, 168,* 1137–1151.

IOC-Intergovernmental Oceanographic Commission. (1997). IUGG/IOC TIME project numerical method of tsunami simulation with the leap-frog scheme. UNESCO, Paris. http://www.jodc.go.jp/info/ioc_doc/Manual/122367eb.pdf. Accessed Jan 2016.

Jiménez, C. (2010). Software para determinación de ocurrencia de maremotos. *Boletín de la Sociedad Geológica del Perú., 104,* 25–31.

Jiménez, C., Moggiano, N., Mas, E., Adriano, B., Fujii, Y., & Koshimura, S. (2014). Tsunami waveform inversion of the 2007 Peru (Mw 8.1) earthquake. *Journal of Disaster Research, 8*(2), 266–273.

Jiménez, C., Moggiano, N., Mas, E., Adriano, B., Koshimura, S., Fujii, Y., et al. (2013). Seismic source of 1746 Callao Earthquake from tsunami numerical modeling. *Journal of Disaster Research, 9*(6), 954–960.

Lay, T., Yue, H., Brodsky, E., & An, C. (2014). The 1 April 2014 Iquique, Chile, Mw 8.1 earthquake rupture sequence. *Geophysical Research Letters, 41,* 3818–3825.

Mas, E., Adriano, B., Kuroiwa, J., & Koshimura, S. (2014a). Reconstruction process and social issues after the 1746 earthquake and tsunami in Peru: Past and present challenges after tsunami events. *InPost Tsunami Hazards, 44,* 97–109.

Mas, E., Adriano, B., Pulido, N., Jimenez, C., & Koshimura, S. (2014b). Simulation of tsunami inundation in Central Peru from future megathrust earthquake scenarios. *Journal of Disaster Research, 9*(6), 961–967.

Okada, Y. (1992). Internal deformation due to shear and tensile faults in a half space. *Bulletin of Seismological Society of America, 82*(2), 1018–1040.

Okal, E. (2009). Excitation of tsunamis by earthquakes, chapter V. In: E. Bernard, A. Robinson (Eds.), The sea: Tsunamis, volume 15 (pp. 137–177). London: Harvard University Press.

Papazachos, B., Scordilis, E., Panagiotopoulos, D., & Karakaisis, G. (2004). Global relations between seismic fault parameters and moment magnitude of Earthquakes. *Bulletin of the Geological Society of Greece, 36,* 1482–1489.

Silgado, E. (1978). Historia de los Sismos más notables ocurridos en el Perú (1513–1974). Boletín N° 3. Instituto de Geología y Minería. Lima, Perú.

(Received April 15, 2016, revised August 25, 2017, accepted August 29, 2017)